A. Khan

D. Ceglarek*

J. Shi

J. Ni

T. C. Woo

S. M. Wu Manufacturing Research Center,
The University of Michigan,
Ann Arbor, Michigan 48109-2136
e-mail: Darek@engin.umich.edu

Sensor Optimization for Fault Diagnosis in Single Fixture Systems: A Methodology

Fixture fault diagnosis is a critical component of currently evolving techniques aimed at manufacturing variation reduction. The impact of sensor location on the effectiveness of fault-type discrimination in such diagnostic procedures is significant. This paper proposes a methodology for achieving optimal fault-type discrimination through an optimized configuration of defined "sensor locales." The optimization is presented in the context of autobody fixturing—a predominant cause of process variability in automobile assembly. The evaluation criterion for optimization is an improvement in the ability to provide consistency of best match, in a pattern recognition sense, of any fixture error to a classified, anticipated error set. The proposed analytical methodology is novel in addressing optimization by incorporating fixture design specifications in sensor locale planning—constituting a Design for Fault Detectability approach. Examples of the locale planning for a single fixture sensor layout and an application to an industrial fixture configuration are presented to illustrate the proposed methodology.

1 Introduction

An automobile is a complex piece of machinery, particularly when considered in the assembly context. The structural frame of the automobile, the Body-In-White (BIW), is made up of up to 800 distinct oriented surfaces. This requires a complement of 150–250 different fixtures with multiple tooling elements to assemble. A complexity consideration such as this coupled with a statistical likelihood of 150 assembly flaws per average production day (or in one of six cars) due to body discrepancies alone, makes it apparent that overall design intent needs to encompass detection and localization of such errors. (Similar complexity in a broader manufacturing context are brought up in Ayres, 1988.) The largest identifiable chunk of all assembly defects, expressed as problems per 100 vehicles, is attributable to process variability in the BIW (J. D. Power, 1994). These account for in excess of 30 percent of all utility vehicle defects. Flaws or error manifestations in cases involving process variability take the form of dimensional variation in the product. A study on the autobody assembly involved in utility vehicle assembly (Ceglarek and Shi, 1995), reveals that as much as 72 percent of all defect root causes are attributable to failures of the assembly fixtures. Such fixture failure modes, present predictable means of assigning *failure types* to specific *part/tooling element failures* in the fixture. This characteristic is of significant help in diagnosis.

While recent advances in fixture design (Asada and By, 1985; Menassa and DeVries, 1989) have resulted in improved fixtures in terms of general design objectives, fixture related dimensional faults continue to be the dominant root cause of flaws directly influencing process variability. This is in spite of concurrent advances in Optical Coordinate Measuring Machine (OCMM) gaging technology for the BIW, which now provides exhaustive per part measurement for 100 percent of parts in critical autobody assembly areas in many plants. Analysis of variability content in the BIW does not require imposition of constraints on the actual positioning of the OCMM laser sensor to accomodate practical considerations such as assembly task requirements etc. Consequently, for purposes of discussion a sensor location is not distinguished from an assigned measurement point location in a sensor locale.

The wealth of dimensional information generated (frequently as many as 100 sensor locations in an OCMM set up for the BIW) presents a challenge on two fronts:

1. *Meaningfulness of Sensor Data:* While exhaustive per part sensor measurement is useful, the information can be put to *meaningful* use in diagnosis only if it conforms to a diagnostic framework designed to:
   (a) exhaustively identify all fault types occurring due to tooling element failures;
   (b) obtain a representation of the signature of each fault type, as registered by a candidate sensor set;
   (c) obtain a sensor set "locale" which highlights the fault causing the largest measure of error; and
   (d) to optimize consistency in obtaining a resulting best match.
2. *Root Cause Localization:* The need is to *synthesize* a sensor pattern of "effect" data and map the result onto the space of "causes" as identified from the geometry and location of tooling elements on the fixture.

The requirement of such a comprehensive root cause isolation and diagnosis methodology is to identify the failure of a single functionality from the set of fixture element functionalities. This is achieved through a sensor reading interpretation in the light of variation patterns—combining 1 and 2 above (Fig. 1).

1.1 Optimal Sensor Layout. Efficient fault isolation hinges on an effective sensor layout. The configuration of the sensor layout becomes relevant when *multiple* sensors are used to provide a comprehensive problem description. Multiple sensor usage usually requires a strategy on sensor data fusion/integration. This has been taken to mean a combination of available state variable estimates used to provide an estimate of a variable (Chryssolouris et al., 1992), or simply the systematic use of such data to assist in a single task (Luo and Lin, 1988). Sensor position optimization has been performed (Tarabanis et al., 1991) to integrate and satisfy vision task requirements with specific depth-of-field or field-of-view type constraints, and, through use of Gaussian maps, to resolve issues of object occlusion.

* Corresponding Author.

Contributed by the Manufacturing Engineering Division for publication in the JOURNAL OF MANUFACTURING SCIENCE AND ENGINEERING. Manuscript received July 1996; revised Oct. 1997. Associate Technical Editor: J. Sutherland.

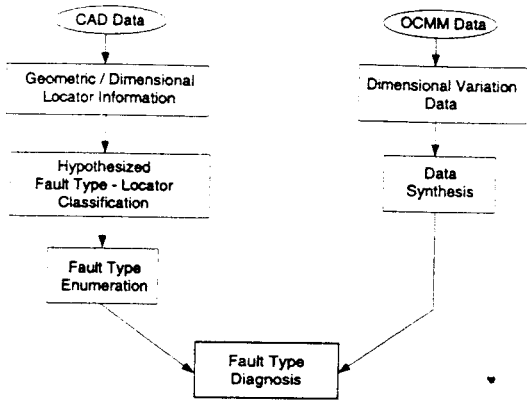

Fig. 1 Root cause isolation: methodology outline

Sensor planning has traditionally taken the form of a search method, a simulation method, or a synthesis approach (Zussman et al., 1994; Cowan and Kovesi, 1988). The first involves a heuristic-based search for (a) sensor location(s), accompanied by tests for the satisfaction of a task related need. The simulation approach utilizes a set of sensor and object scenario descriptions to converge on a satisfactory sensor distribution. The approach in the synthesis method is to utilize a set of specified constraints on the task to analytically arrive at a constraint-fulfilling solution, which may then be deemed an optimal configuration. The approach outlined here combines elements of all of these approaches in that object and sensor descriptions are used as the basis; constraints on sensor locations are introduced to avoid "blacked-out" areas (ineligible as a sensor locale due to manufacturing/design constraints), and there is the option of heuristic use to limit locales through a constriction of the optimization space. However, sensor synthesis for diagnosis has certain unique requirements. While a method of describing the location of an assembled part is still required; *location* is no longer viewed as a unique or optimal position, but as the range of positions which, as dimensional variation, represents a specific fault type. Most current implementations utilize an approach which corresponds loosely to one proposed by Shekhar et al. (1988) for object localization, coupled with the use of engineering judgement to determine feasibility.

1.2 Problem Generality Considerations. The problem which Shekhar et al.'s object localization addresses (that of localizing an object as in a manipulator end-effector, utilizing sensory information), diverges from part-fixturing in certain crucial aspects:

1. BIW components have arbitrary shapes, often not amenable to quadrangle form representations.
2. Location of measurement points cannot, for practical reasons, be artificially constrained to corner points;
3. Failure patterns can be arbitrary combinations of translations or rotations in 3-D space, not necessarily a single rotation of the component.

While their conclusions remain valid for object localization, force fitting this method to fixture fault localization is not feasible. The approach proposed here provides an effective solution when few simplifying assumptions can be made regarding either part/fixture geometry or fault nature/complexity.

2 Problem Setting: Autobody Part Fixturing

A part fixture serves to ensure locational and clamping stability, deterministic part location, and total restraint. A fixture under evaluation may be deemed "correct" if these conditions are met, as has been shown in Asada and By (1985). To estimate the extent of realization of these desirable characteristics, we characterize the fixture through defining a layout of Tooling Elements (TE), which include locating pins (P) and block locators with clamps (C). The totality of Ps and Cs are responsible for "correct" fixture function and thus for dimensional repeatability of parts in assembly operations. For the rigid part, the layout used is based on the 3-2-1 principle. The principle provides for part motion constraint through the use of three groups of locators laid out in two orthogonal planes, as shown in Fig. 2. These serve to achieve

1. a combination of X and Z direction constraints in the primary (XZ) plane, through a fixed diameter or conical (four-way constraint providing), locating pin P_1;
2. a unidirectional (Z) constraint, through the (two-way constraint providing) pin P_2 in the primary plane;
3. a Y direction constraint, through the set of block locators (C_1, C_2, C_3) on the secondary (YZ) plane.

2.1 Fixture Faults. Tooling faults are directly attributable to one or a combination of failure conditions associated with each of the TEs. Such TE fault conditions are in turn a direct cause of part mislocation in assembly. TE faults have been found to be of both the inherent-in-design and the developed-through-process-life forms. Instances of the former include poor clamp design/manufacture, block locator-clamp mating mismatches and off-dimension locating pins. Failures of the latter form may occur from locator wear, inclusions on and pitting of mating surfaces, and degradation in applied clamp pressure levels due to part fatigue over time.

A part-control axis for a TE defines a critical direction for that TE. TEs may offer redundant control along certain axes, as has been seen (in the case of the Z axis above). In this context Complementary Tooling Elements (CTE) may be defined as the set of constraint providing complements to a given Tooling Element (TE) for a specified axis Ξ. This is the subset of TEs constraining motion along Ξ, with excludes the TE under consideration.

Fixture faults can be defined in terms of the influence exerted by CTEs on part location in the event of a TE failure. Succinctly put, part mislocation due to a TE fault is defined by the CTEs of a TE in the Ξ axis. This is immediately obvious from the observation that when a TE controlling a certain axis on a rigid part fails, then the extent of the dimensional mislocation is determined by all other TEs controlling that axis. An analysis of fault types (Ceglarek and Shi, 1996) leads to the following generalized fault induced resultant motion:

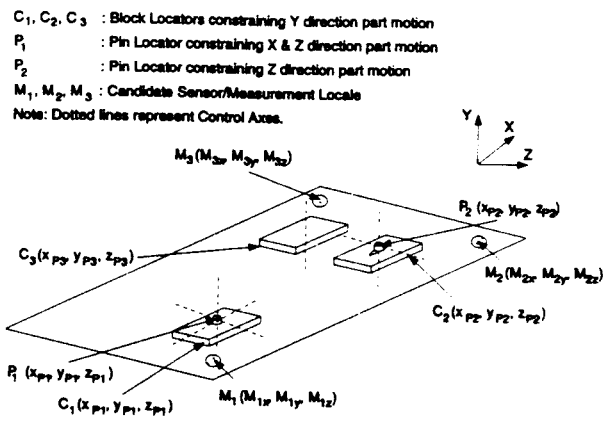

Fig. 2 3-2-1 fixture layout

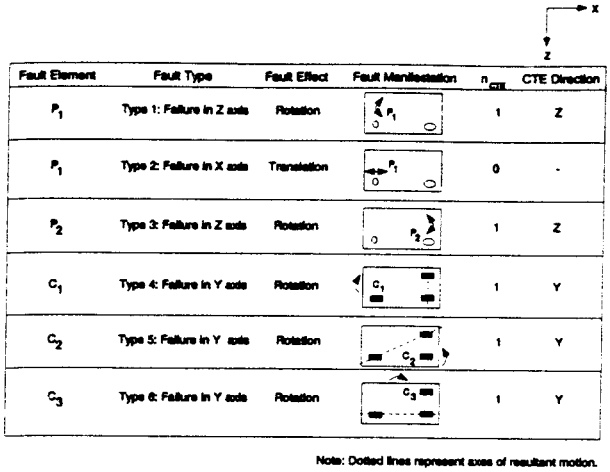

Fig. 3 3-2-1 fault manifestations

1. resultant translation along the Ξ axis—if the complementary tooling elements to TE (n_{CTE}) is 0;
2. resultant rotation along the axis defined by one complementary tooling element—if the complementary tooling elements to TE (n_{CTE}) is 1; and
3. resultant rotation along the axis defined by two complementary tooling elements—if the complementary tooling elements to TE (n_{CTE}) is 2.

These fault manifestations are summarized in Figure 3; arrows indicating the direction of resultant part motion.

2.2 Fault Classification and Diagnosis. The dimensional extent of the fault as captured by a sensor layout is a function of fault severity as well as the geometry of the layout of the sensors and TEs on the fixture. A fault signature may be defined for each fault type in terms of a particular TE layout and a sensor locale. A "sensor locale" is defined as the complete set of XYZ coordinate descriptions of sensors associated with the fixture constituting a candidate layout. The generalized fixture of Fig. 2 provides the basis for a generic fault type categorization:

Type 1 Fault: P_1 failure in the Z control axis;
Type 2 Fault: P_1 failure in the X control axis;
Type 3 Fault: P_2 failure in the Z control axis;
Type 4 Fault: C_1 failure in the Y control axis;
Type 5 Fault: C_2 failure in the Y control axis;
Type 6 Fault: C_3 failure in the Y control axis.

Three axis measurements at each of three sensor locations, provides nine sensor variable measures. A set of diagnostic vectors can now be defined as the set of (sensor) vectors associated with each of these faults for a given tooling configuration and sensor locale. A diagnostic vector (Ceglarek and Shi, 1996)

$$\mathbf{d(i)} = (d_{i1}, \ldots, d_{ni})^T \tag{1}$$

has n entries (where n is the number of sensor variable measures) describing a variation pattern caused by a type i fault. Elements d_{ij}, $(j = 1, \ldots n)$ represent a ratio of the standard deviation in a component direction to the overall sensor standard deviation associated with the fault type. If χ_j represents the measured variable, then:

$$d_{ji} = \frac{\sigma_{\chi_j}}{\sigma} \quad \text{for} \quad j = 1, \ldots, n \tag{2}$$

where σ_{χ_j} is the standard deviation of variable χ_j, and $\sigma = \sqrt{\sum_{j=1}^{n} \sigma_{\chi_j}^2}$.

OCMM measurements, reflecting dimensional behavior of the BIW assembly, are described by measurement vectors $[\chi_1, \chi_2, \ldots \chi_n]_t$, where t represents the number of measured automotive bodies. $\chi_1, \chi_2, \ldots \chi_n$ are measures of deviation from nominal on each of the t bodies—an inherent measure of fault trends in the fixturing, (e.g. faults involving repeatability about some, non-nominal, mean). The set of diagnostic vectors can be represented as a single diagnostic matrix $\mathbf{D}$; which for the generic 3-2-1 fixture of Fig. 2, takes the form:

$$\mathbf{D} = \mathbf{d}(1), \mathbf{d}(2), \ldots, \mathbf{d}(6) \tag{3}$$

$$= \begin{bmatrix} d_{11} & d_{12} & \cdots & d_{16} \\ d_{21} & d_{22} & \cdots & d_{26} \\ \vdots & \vdots & \vdots & \vdots \\ d_{n1} & d_{n2} & \cdots & d_{n6} \end{bmatrix} \tag{4}$$

The index taking values $1, \ldots, 6$ in the second subscript of the matrix elements in Eq. (4) corresponds to the six fault types, and the first subscript indexes the $i = 1, \ldots, n$ sensor variable measures. For the $n = 9$ sensor variable measures (for three sensors each with three axis measurements) in the generalized fixture configuration, the measurement vector $\boldsymbol{\chi}$ based on all sensors M_i $(i = 1, 2, 3)$ may be expressed as:

$$\boldsymbol{\chi} = [\chi_1\ \chi_2\ \chi_3\ \chi_4\ \chi_5\ \chi_6\ \chi_7\ \chi_8\ \chi_9] \tag{5}$$

$$= [M_{1x}\ M_{1y}\ M_{1z}\ M_{2x}\ M_{2y}\ M_{2z}\ M_{3x}\ M_{3y}\ M_{3z}] \tag{6}$$

Vectors $\mathbf{d(i)}$ can be obtained in terms of the dimensional measures of the tooling layout and the sensor locale. These are provided here without derivation, but can be obtained through relating Eq. (2) with the component direction dimensional motions and the corresponding resultant component direction stan-

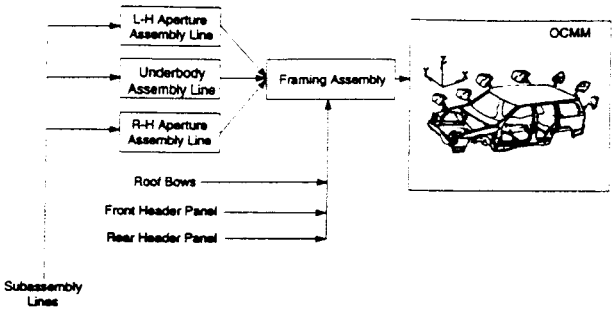

Fig. 4 Framing assembly process schematic

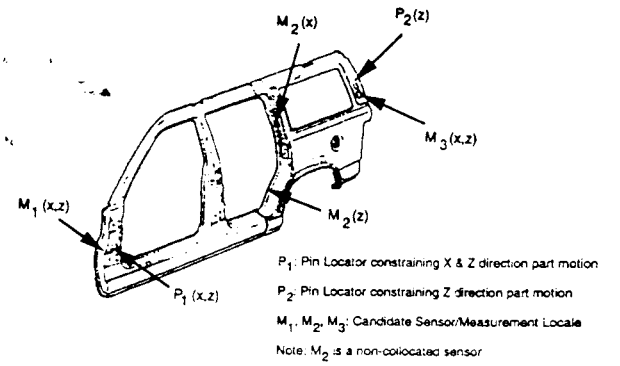

Fig. 5 L-H aperture pin and sensor layout

dard deviations for the generic case of Fig. 2 (Ceglarek and Shi, 1996). The standard deviation components of the $\mathbf{d}(\mathbf{i})$ being proportional to distance measures, they can be expressed in the form:

$$\mathbf{d}(1) = (d_{11} \quad d_{21} \quad d_{31} \quad d_{41} \quad d_{51} \quad d_{61} \quad d_{71} \quad d_{81} \quad d_{91})^T$$
$$= \frac{[z(P_2, M_1) \quad 0 \quad x(P_2, M_1) \quad z(P_2, M_2) \quad 0 \quad x(P_2, M_2) \quad z(P_2, M_3) \quad 0 \quad x(P_2, M_3)]^T}{\sqrt{d^2(P_2, M_1) + d^2(P_2, M_2) + d^2(P_2, M_3)}} \quad (7)$$

$$\mathbf{d}(2) = (d_{12} \quad d_{22} \quad d_{32} \quad d_{42} \quad d_{52} \quad d_{62} \quad d_{72} \quad d_{82} \quad d_{92})^T$$
$$= [0.577 \quad 0 \quad 0 \quad 0.577 \quad 0 \quad 0 \quad 0.577 \quad 0 \quad 0]^T \quad (8)$$

$$\mathbf{d}(3) = (d_{13} \quad d_{23} \quad d_{33} \quad d_{43} \quad d_{53} \quad d_{63} \quad d_{73} \quad d_{83} \quad d_{93})^T$$
$$= \frac{[z(P_1, M_1) \quad 0 \quad x(P_1, M_1) \quad z(P_1, M_2) \quad 0 \quad x(P_1, M_2) \quad z(P_1, M_3) \quad 0 \quad x(P_1, M_3)]^T}{\sqrt{d^2(P_1, M_1) + d^2(P_1, M_2) + d^2(P_1, M_3)}} \quad (9)$$

$$\mathbf{d}(4) = (d_{14} \quad d_{24} \quad d_{34} \quad d_{44} \quad d_{54} \quad d_{64} \quad d_{74} \quad d_{84} \quad d_{94})^T$$
$$= \frac{[0 \quad d(C_{23}, M_1) \quad 0 \quad 0 \quad d(C_{23}, M_2) \quad 0 \quad 0 \quad d(C_{23}, M_3) \quad 0]^T}{\sqrt{d^2(C_{23}, M_1) + d^2(C_{23}, M_2) + d^2(C_{23}, M_3)}} \quad (10)$$

$$\mathbf{d}(5) = (d_{15} \quad d_{25} \quad d_{35} \quad d_{45} \quad d_{55} \quad d_{65} \quad d_{75} \quad d_{85} \quad d_{95})^T$$
$$= \frac{[0 \quad d(C_{13}, M_1) \quad 0 \quad 0 \quad d(C_{13}, M_2) \quad 0 \quad 0 \quad d(C_{13}, M_3) \quad 0]^T}{\sqrt{d^2(C_{13}, M_1) + d^2(C_{13}, M_2) + d^2(C_{13}, M_3)}} \quad (11)$$

$$\mathbf{d}(6) = (d_{16} \quad d_{26} \quad d_{36} \quad d_{46} \quad d_{56} \quad d_{66} \quad d_{76} \quad d_{86} \quad d_{96})^T$$
$$= \frac{[0 \quad d(C_{12}, M_1) \quad 0 \quad 0 \quad d(C_{12}, M_2) \quad 0 \quad 0 \quad d(C_{12}, M_3) \quad 0]^T}{\sqrt{d^2(C_{12}, M_1) + d^2(C_{12}, M_2) + d^2(C_{12}, M_3)}} \quad (12)$$

where $z(P_2, M_1)$, $x(P_2, M_1)$, etc., represent component distances from P_2 to M_1 along axes Z and X respectively, and where $d(C_{12}, M_1)$, $d(C_{12}, M_2)$, etc., represent the shortest (perpendicular) distance from M_1, M_2 to the axis joining C_1 and C_2, respectively. All distance measures are computed in a Euclidean distance sense, with the distance measure between points a and b being computed as $d(a, b) = \sqrt{(x_a - x_b)^2 + (y_a - y_b)^2 + (z_a - z_b)^2}$. Thus, for a set of tooling layouts and sensor locales, it is possible to obtain a descriptively complete matrix representation of all associated tooling faults. Data synthesis to obtain a set of points which have high fault magnitude, may be carried out through a point-by-point estimate of data variation for each sensor variable in the form of a 6-sigma value, $\sigma_\chi = \sqrt{\sum_{i=1}^{N}(\chi_i - \bar{\chi})^2/(N-1)}$, and where χ_i is the ith measurement from a sensor and $\bar{\chi}$ the mean of the sample size N values.

A second requirement is to group measurements based on a single root cause from within the sensor data set. This is based on a covariance analysis. For data pairs, say χ_i and ζ_i, elements of covariance matrix $\mathbf{Q}$

$$\mathrm{Cov}_{\chi,\zeta} = \frac{\sum_{i=1}^{N}(\chi_i - \bar{\chi})(\zeta_i - \bar{\zeta})}{\sqrt{\sum_{i=1}^{N}(\chi_i - \bar{\chi})^2 \sum_{i=1}^{N}(\zeta_i - \bar{\zeta})^2}} \quad (13)$$

for a sample of size N, with $\bar{\chi}$ and $\bar{\zeta}$ representing data means over the N samples. Measurements exhibiting a high covariance measure may be grouped together. The rationale is that strong covariances are indicative of variations linked to a single root cause.

If $\boldsymbol{\chi} \in \mathbf{R}^n$ represents N measurements from the n sensors with matrix $\mathbf{Q}$, then we can define $\tilde{\boldsymbol{\chi}} \in \mathbf{R}^p$ for p, as a transformation of $\boldsymbol{\chi}$ such that $\tilde{\boldsymbol{\chi}} = \boldsymbol{\chi}\mathbf{A}$; where $\mathbf{A} = [a_{ij}]_{n \times n}$, with $\boldsymbol{\chi}$ defined as in Eq. (5). The ith column of $\mathbf{A}$, represented as $\mathbf{a}_i = [a_{i1} \ldots a_{in}]^T$, is the ith eigen vector of $\mathbf{Q}$, obtained as:

$$[\lambda_i \mathbf{I} - \mathbf{Q}]\mathbf{a}_i = 0 \quad i = 1, \ldots, n \quad (14)$$

where λ_i is the eigen value of the ith principal component, $\mathbf{I}$ is the identity matrix, and $\mathbf{a}_i$ is the ith eigen vector corresponding to λ_i. The predominant fault, modeled based on sensor M_1, M_2, M_3 measures, is described by a first eigen value-eigen vector pair $(\mathbf{a}_1, \lambda_1)$ (Ceglarek and Shi, 1996)—functions of $\mathbf{d}(\mathbf{i})$, obtained in Eqs. (7)–(12). The first eigen vector points in the direction of the greatest variability in the data, and the orthogonal projection of the data onto this eigen vector is the first eigen value.

2.3 A Case In Point: An Industrial Fixturing Configuration. The problem and the solution method are best illustrated in the context of industrial fixturing, such as those utilized as part of the framing operation in automobile assembly. The major assembly task in autobody framing assembly is performed at a framing station where the vehicle underbody is welded to the R-H and L-H apertures (the Right and Left aperture assembly lines) and the Roof Bows (Fig. 4).

A Geometric (position-setting) station is utilized for each of the subassemblies involved, including the L-H aperture. The L-H aperture fixture was utilized as a test fixture for ongoing analysis and optimization, as it is characteristic of the generalized class of n-2-1 fixture layouts. Also, the relatively large part size and weight of the fixtured sheet metal increases sensitivity to TE-induced errors. L-H aperture fixturing assumes completed welds and deterministic part location in other fixtures in assembly which locate its subcomponents. The associated CAD system layout and the corresponding candidate sensor locale set is shown in Fig. 5.

The aim of the diagnostic procedure is to first identify the failure patterns and then utilize these to isolate a fault root cause. Mathematically, the optimal set may be obtained through a procedure involving constrained iterative maximization. The distance between failure patterns represented by the diagnostic vector, $\mathbf{d}(\mathbf{i})$, is maximized for different sensor locale sets. This diagnostic vector is equivalent to the dominant eigen vector computed for the measurement data as Eq. (14) from $\mathbf{Q}$ [Eq. (13)]. Each fault is manifest as a variation pattern based on

measurement from all sensors in a locale set, and described by eigen vector $\mathbf{a}_1$.

3 Optimization

An optimal sensor location can be obtained by *maximizing* the distance between each dominant eigen vector, obtained for each of the tooling faults. The connotation of the maximization premise is to increase the power, or the degree of reliability, of the discriminant. The discriminant may be viewed in a transformation setting, as a mapping from the dimensional pattern space to the fault type *attribute* space. Here the discriminant serves in a pattern recognition sense, as an estimator of the fault type class membership of an observed or hypothesized fault type identified in dimensional space. Efficient fault discrimination is thus possible if the sensor locale provides a maximal spread of fault type classes in space. In the event of sensor noise or multiple fault type coexistence, the primary fault type associated with the prominent eigen vector can be readily distinguished.

3.1 The Diagnosability Index. A diagnosibility index is proposed which quantifies the ability of the system, with sensors at a candidate sensor locale, to isolate faults. The diagnosability or fault isolation index J, may be defined as a function of the minimum distance between pairs of diagnostic vectors, $\mathbf{d}(\mathbf{i})$ $i = 1, \ldots 6$ [Eqs. (7)–(12)], over all such pairs:

$$J = \forall_{i \neq j} \min \sum_{i=1,\ldots 6} \sum_{j=1,\ldots 6} \|\mathbf{d}(\mathbf{i}) - \mathbf{d}(\mathbf{j})\| \qquad (15)$$

The index J is thus an estimate of the closest pairing of fault type manifestations (in fault space) for a candidate sensor locale. The desirability criteria can now be formulated in terms of a search in dimensional space for a sensor locale, which when mapped into fault space, results in the maximization of J. The $\{\mathbf{d}(\mathbf{i}), \mathbf{d}(\mathbf{j})\}$ pair, corresponding to smallest Euclidean distance, varies during the iterative search procedure. This represents a search for the "maximal spread" referred to earlier. The problem may be succinctly formulated as a constrained optimization, where the objective function is sought to be maximized subject to inequality constraints:

$$J_{\text{opt}} = \forall_{i \neq j} \max \left[\min \sum_{i=1,\ldots 6} \sum_{j=1,\ldots 6} W_{ij} \|\mathbf{d}(\mathbf{i}) - \mathbf{d}(\mathbf{j})\|\right]$$

$$\text{s.t. } G(x, y, z) \leq 0 \qquad (16)$$

$G(x, y, z)$ represents the constraint set on sensor locations corresponding to "blacked-out" areas on the fixture alluded to earlier. Constraints can be formulated from CAD data to directly reflect positions on the fixture which for one reason or another may be infeasible as a candidate sensor locale. The optimization as proposed is generic to 3-2-1 fixtures; weights W_{ij} are introduced to provide fixture-specific control on the relevance of specific tooling faults to the fixture under consideration. These may take on binary (1/0) values, to reflect the absence of a certain fault type in a configuration; or real values, to represent the relative importance of the detection of a certain fault type, constituting a Design for Detectability. This design approach complements design for the fundamental function of part positioning, accomplished through conventional TE selection, to ensure a stable part location. To provide an optimal level of detectability, an optimal sensor locale plan is incorporated into the design, using the designed TE locations to guarantee the best level of fault type detection and isolation. By utilizing the J_{opt} index, the spread and location of the $\mathbf{d}(\mathbf{i})$ are optimized to obtain such a locale.

Optimization on the J_{opt} index is implemented using a set of functions from the Matlab (Matlab, 1994) toolbox, implementing a Sequential Quadratic Programming method (the code running in a Solaris Unix environment on a Sun SPARC 20). The optimization performance of the functions is seen to be robust to changes in the starting set in terms of convergence, with problems of consistency as due to local minima in the multi-dimensional space not being encountered. A block diagram of the optimization implementation is shown in Fig. 6.

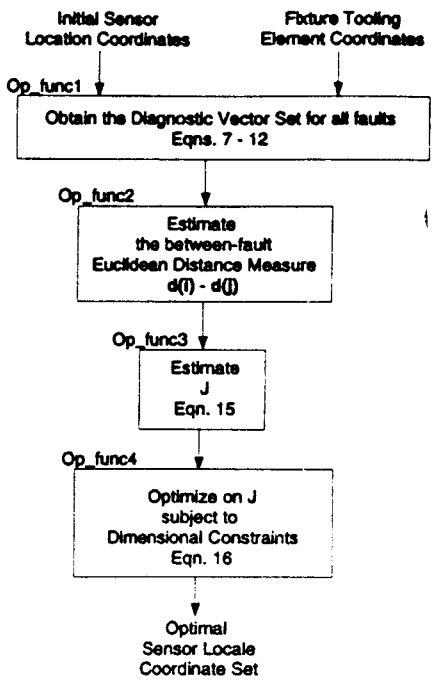

Fig. 6 3-2-1 optimization implementation: outline

3.2 Sensor Noise Considerations. The fundamental premise of optimization on the discrimination function is that the mapping of the predominant sensor-based fault (obtained as the first eigen value-eigen vector pair of the covariance matrix $\mathbf{Q}$) on the appropriate $\mathbf{d}(\mathbf{i})$ be made as invariant as possible to noise in the set χ. Optimization to achieve a maximization on J_{opt} (Op_func4 in Fig. 6) has the effect of maximizing the overall dispersion of diagnostic vectors $\mathbf{d}(\mathbf{i})$, for all i. For example, a design for a specific noise-insensitivity is frequently required to best isolate a *specific* fault vector, $\mathbf{d}(\mathbf{i})^0$, in the face of sensor noise.

If $\mathbf{a}_1$ is the eigen vector corresponding to the first eigen value of the covariance matrix $\mathbf{Q}$ [Eq. (14)], then the objective is to ensure high fault match efficiency of the specific $\mathbf{d}(\mathbf{i})^0$ with unknown fault eigen vector $\mathbf{a}_1$:

$$\min \|\mathbf{a}_1 - \mathbf{d}(\mathbf{i})^0\|^2 \qquad (17)$$

which is equivalent to maximizing the discriminant function $g(\mathbf{a}_1)$ (Fukunaga, 1972), where:

$$g(\mathbf{a}_1) = [\mathbf{d}(\mathbf{i})^0]^T \mathbf{a}_1 - \tfrac{1}{2} \|\mathbf{d}(\mathbf{i})^0\|^2 \qquad (18)$$

for the specific $\mathbf{d}(\mathbf{i})$. A discriminant function for identification of a fault type with sensors subject to noise, η, has been proposed in Ceglarek (1996):

$$\eta = 2|g(\mathbf{a}) - g(\mathbf{d}(\mathbf{i}))| \times 100\% \qquad (19)$$

to estimate if identification of a type $\mathbf{i}$ fault (for a specific $\mathbf{d}(\mathbf{i})$) is robust to the sensor noise. Robustness levels are considered adequate if the attained discriminant (η) satisfies $\eta \leq \eta_0$, where η_0 depends on the variability of the fault. An η_0 value of 0 percent would correspond to zero noise robustness, requiring a faithful manifestation of $\mathbf{d}(\mathbf{i})$ by the sensor set for fault identification. As η_0 approaches 50 percent, corresponding to a theoretical maximum robustness, noise levels increasingly drive up the probability of a misinterpretation of a fault manifestation as a

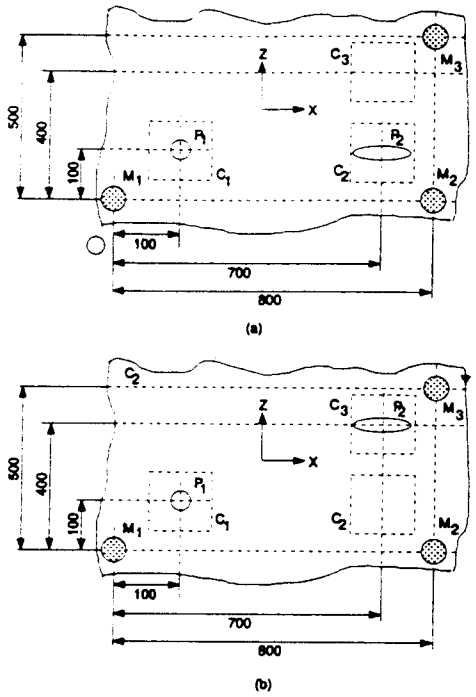

Fig. 7 (*a*) Candidate fixture geometry (*b*) an alternative geometry

neighboring fault type, instead of as $\mathbf{d}(\mathbf{i})$. An estimate can be obtained of increase in the threshold level η_0 for $\mathbf{d}(\mathbf{i})$, given $\mathbf{i}$, as a consequence of optimization. This may be considered an enhancement of discriminant $g(\mathbf{d}(\mathbf{i})^0)$:

$$g(\mathbf{d}(\mathbf{i})') - g(\mathbf{d}(\mathbf{i})^0) \tag{20}$$

where $\mathbf{d}(\mathbf{i})'$ is a vector obtained as:

$$\min \|\mathbf{d}(\mathbf{j}) - \mathbf{d}(\mathbf{i})^0\| \quad \forall j \neq i \tag{21}$$

This is performed as a sub-optimization (as Op-func2 in Fig. 6), on Euclidean distance for a fixed i. An example of the implication of optimization for a threshold level increase in fault detection is provided in the next section.

4 Scenarios

Two example scenarios are presented here to illustrate the outlined procedure. The first involves an implementation of the sensor locale selection approach on the familiar 3-2-1 configuration with assigned positions of TEs, and starting from a prior experience-based, informed choice of sensor positions. This candidate sensor locale was chosen to correspond loosely to the locations chosen for sensor positioning in industrial fixtures of this configuration. The second example involves the implementation of the algorithm to the L-H aperture framing station fixture in a utility vehicle assembly line. Geometrical data corresponding to the critical features on the fixture are as represented in a CATIA-Solid Modeler[1] design environment.

4.1 An Example of Sensor Planning in the Generic 3-2-1 Case. In this example a set of TEs consisting of 3 block locators, a single one-way locator, and one two-way locator are chosen. The initial sensor layout with this TE configuration is shown in Fig. 7(*a*). We aim to obtain the coordinate measures $M_{1,(x,y,z)}$, $M_{2,(x,y,z)}$, $M_{3,(x,y,z)}$ corresponding to the optimal sensor locale.

[1] Computer-graphics Aided Three-dimensional Interactive Application—a design environment developed by Dussault Systems, France, and supported by IBM.

Table 1 Generic fixture (*A*) optimization results

Coordinate	*Initial Sensor Locale*	*Optimal Sensor Locale*
M_{1x}	50.0	79.42
M_{1z}	50.0	101.261
M_{2x}	850.0	856.24
M_{2z}	50.0	153.23
M_{3x}	850.0	712.03
M_{3z}	550.0	335.37

The measure of the fault isolation (diagnosability) index for the informed guess candidate sensor locale (minimum distance of fault type pairings) was first obtained as:

$$J_{\text{init}} = 1.4770 \tag{22}$$

The optimization procedure was carried out utilizing the Matlab function sets for constrained multivariables (Nelder and Mead, 1965; Powell, 1978). Results of optimization are in Table 1. The optimized sensor locale is seen to be in the area of the informed guess location for sensors M_1 and M_2, but not for M_3. The new J:

$$J_{\text{opt1}} = 1.8515 \tag{23}$$

corresponds to an approximately 25 percent improvement in the overall fault isolation. The J_{opt} index reflects the pessimistic (worst-case) scenario, in terms of isolating the closest $\{\mathbf{d}(\mathbf{i}), \mathbf{d}(\mathbf{j})\}$ eigen vector pairing, should both faults represented by the vector pair exist on the fixture.

Additional runs were performed with a change in TE positions to correspond to an alternative part-holding scheme providing the same part-holding functionality. For this configuration, shown in Fig. 7(*b*), (results in Table 2), the corresponding J_{init}:

$$J_{\text{init2}} = 1.2131 \tag{24}$$

and J_{opt}:

$$J_{\text{opt2}} = 1.6507 \tag{25}$$

For all fault pairings, the level of worst-case isolation achieved (J_{opt2}) is lower than that for the original. These results (Fig. 8) provide additional insights into the influence of fixture design on fault isolation performance. A significant performance difference is registered between results corresponding to J_{opt1} and J_{opt2}. The original TE configuration performs approximately 53 percent better when compared to the unmodified alternative configuration.

The extent of this improvement in fault detection capability can be explained using an analysis in terms of the noise robustness consideration. As an example, consider the case of a Type 3 fault involving the failure of locating pin P_2 in the generic fixture configuration. This causes variation in the entire component part. Corresponding to J_{init1}, the diagnostic vector closest to fault type 3 is found to be fault type 1, with a corresponding estimate of

Table 2 Generic fixture (*B*) optimization results

Coordinate	*Initial Sensor Locale*	*Optimal Sensor Locale*
M_{1x}	50.0	0.76
M_{1z}	50.0	204.07
M_{2x}	850.0	873.76
M_{2z}	50.0	204.07
M_{3x}	850.0	873.77
M_{3z}	550.0	511.46

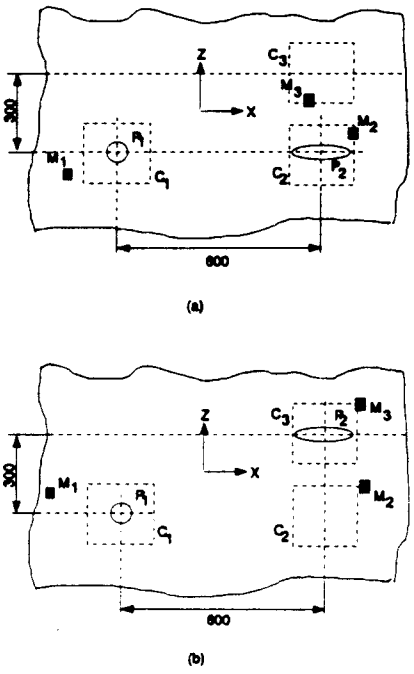

Fig. 8 Optima for the (*a*) candidate fixture geometry (*b*) alternative geometry

$$g(\mathbf{d}(\mathbf{i})^0) = 1.6172 \tag{26}$$

This can be intuitively appreciated as Type 1 and Type 3 faults both cause rotations in the Z axis. After optimization on sensor locale, corresponding to an overall J_{opt} measure of 1.8515, we obtain:

$$g(\mathbf{d}(\mathbf{i})') = 1.8574 \tag{27}$$

This corresponds to an enhancement, in Euclidean distance terms, of 0.2402 or 14.9 percent (Eqs. 23, 27).

As noted, the worst-case effect of noise on the sensors is the identification of the closest pairing of Type 1 fault in lieu of Type 3. A new boundedness estimate can now be placed on the threshold of η, as, in the worst case, the increase in η_0 now tolerable due to J_{opt}. The new η_0 is thus:

$$\eta_0' = 1.149\eta_0 \tag{28}$$

The implication is that an enhanced level of noise insensitivity to Type 3 faults is now achievable. A common, experience-based choice of η_0 is 40 percent, a conservative estimate on the 50 percent exact bisector of the fault types in space. Under normal circumstances, noise levels which cause the vectors to push the bisecting envelope by approaching 50 percent on either side would lead to frequent misidentification of fault types. An optimized sensor locale now allows for identical fault discriminatory capabilities as before and correct fault classification to up to 46 percent.

Ceglarek (1996) derives a relation linking η_0 and the 6-sigma of allowable sensor noise. The graphical study reveals that at the 40 percent upper limit, allowable design noise for the component sensors is 1.734 mm for the generic fixture configuration. It follows that the enhanced η_0' raises allowable design noise to 1.917 mm, an increase of 11 percent. It is also apparent that particular configurations of TEs offer better fault isolation properties in conjunction with an optimal sensor locale than others. This underscores the importance of fixturing design, not merely to achieve efficient part holding, but also for efficient design for detectability.

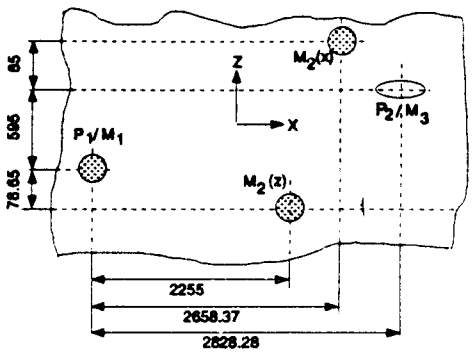

Fig. 9 Geometry and sensor location for the L-H aperture fixture

4.2 Sensor Locale Optimization for the L-H Aperture. The "real-world" L-H Aperture fixturing can be similarly optimized, accommodating requirements peculiar to the configuration. The configuration of an initial candidate sensor locale with the CATIA TE configurations (corresponding to Fig. 5) for two approaches to optimization is shown in Fig. 9. Unlike the generic cases where all sensors provided a complete (three coordinate) measurement set, OCMM sensors often provide unidirectional measurements at certain locations. Sensor M_2 is an instance of this, where physically noncollocated measures are provided at sensor locations $M_2(x)$ and $M_2(z)$, giving unidirectional X and Z measures, respectively. Two independent optimizations were carried out. The first involved a rearrangement of such existing unidirectional measurement sensors to obtain an optimal locale. Unidirectional sensor usage is usually a solution to a manufacturing (especially fixture-specific) constraint on sensor locations at certain measurement points. Conventional multidirectional sensors may still be used in areas other than those "blacked-out" for such measurement. The second optimi-

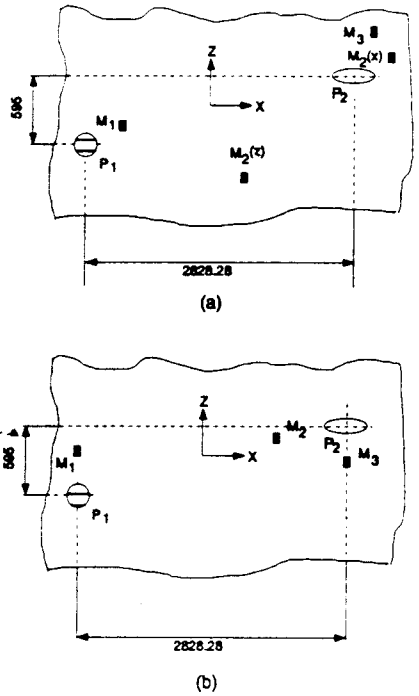

Fig. 10 Optima for the L-H aperture fixture (*a*) noncollocated sensor optimization (*b*) collocated sensor optimization

Table 3 L-H aperture fixture optimization results

Coordinate	Initial Sensor Locale	Optimal Sensor Locale 1	Optimal Sensor Locale 2
M_{1x}	50.0	127.05	50.05
M_{1z}	128.65	191.53	423.93
M_{2x}	2708.37	3036.5	2699.90
M_{2z}	808.65	819.66	616.98
M_{3x}	2878.28	3021.85	2878.30
M_{3z}	723.65	1103.61	384.34
M_{4x}	2305.0	2180.96	-
M_{4z}	50.0	55.3	-

zation approach provides an optimal sensor locale utilizing a complement of such multidirectional sensors, subject to constraints on the optimization reflecting explicitly the existence of such blacked-out areas.

Though differing in implementation detail, the first optimization can be carried out in conceptually identical fashion to the generic case, through accomodating $M_2(z)$ as an additional member of the sensor locale set (identified as M_4) and changing the diagnostic vector representation of Eqs. (7)–(12) to reflect a unidirectional measure from each of two sensors. The J_{init} for this configuration was obtained as:

$$J_{\text{init}} = 1.4947 \tag{29}$$

The results obtained from the optimization (Fig. 10) reveal a correspondence to the original intuitive layout (as suggested in Shekhar et al., 1988), requiring that sensors be placed at part extremities, as can be seen from the X values in Table 3, but balanced with a spatial spread in the Z direction to ensure that Type 1 and 2 faults are effectively distinguishable. The corresponding J_{opt} is:

$$J_{\text{opt1}} = 1.6619 \tag{30}$$

This corresponds to an 11 percent improvement in resultant diagnosability over the trial-and-error based intuitive sensor distribution. As can be seen from Table 3, the optimized locale differs significantly from the existing configuration in the x positioning assigned to M_1. A smaller x coordinate value allows for an increased detectability of an inadequate Z constraint imposed by P_1. The $M_2(z)$, M_3 positioning serves the identical function for the P_2 failure type, while $M_2(x)$ in combination with the other sensors, describes an X direction constraint failure. The optimal layout for M_2, M_3 and M_4 bears out in large part the designer's experience-based decision on sensor location, only repositioning sensors around the original locale to better distribute the fault vectors in space.

The second optimization approach utilizing a set of three multidirectional sensors (closer to the generic implementation of the previous section, but with the imposition of location constraints) provided a higher J_{opt}—with a 30 percent diagnosability improvement—for sensors configured at its optimal locale (Table 3):

$$J_{\text{opt2}} = 1.9481 \tag{31}$$

While the constraints on sensor position alter the optimal sensor layout, this configuration retains the characteristic of a small x for M_1, which along with M_2, monitors X direction failures.

This example addresses a widely felt need in current auto assembly measurement practice, to provide a systematic means of distributing the OCMM laser sensors without resorting to tedious iterations on sensor placement to distinguish between a few test-sample-error-types for the fixture. The method is even more attractive in this context, as it offers an efficient means of addressing the sensor locale problem for a complete list of error types for the fixture. The example optimizations were performed with equal weight placed on all error types; i.e., optimizing on the basis that it is equally important to our purpose, to distinguish between errors of all different class types. Even at this level of generality, it is apparent that significant improvements can be made in fault diagnosis and in implementing root cause solutions with the procedure. In practice, it is usually true that some fault types are more likely to occur than others, or alternatively, that some faults are immediately obvious from a fixture study without resorting to sensor-based data. This suggests that further diagnosability improvements can be anticipated by suitably weighting the fault types in the optimization as needed.

5 Summary and Conclusions

Ensuring the dimensional integrity of complex assembled parts, such as the automobile BIW, has assumed critical importance in modern assembly. The efficiency of fixture diagnosis techniques, utilized to diagnose dimensional faults, is contingent on appropriate and precise sensor-based measurement. A new formalized means of configuring dimensional sensors for efficient and optimal fault type diagnosis in part fixturing has been proposed here. An *optimal sensor locale* methodology has been defined through estimating a maximal Euclidean distance spread of fault types in space, to provide an efficient classification of a manifest fault. The optimization function used in the approach displays a useful resiliency to initial value assumptions, converging to repeatable optima (insensitive to the starting parameter set choice). The classification is based on an exhaustive fault type set proposed for the fixture in the form of a Diagnostic Matrix. The examples demonstrate the utility of the technique in sensor planning, both for conventional generic sensor/fixture types, and in OCMM-based sensing. This allows for systematic planning without taking recourse in the prevalent trial and error or judgment-based approaches. In addition, significant improvements in diagnosability over existing fixture configurations, from the use of the optimal sensor locale configuration, were shown. This approach also addresses the developing need to provide a rapid layout plan in an assembly system, to improve the information content of data available from the emerging trend towards 100 percent measurement of sheet metal assembly.

5.1 Acknowledgments. The authors wish to acknowledge the support of National Science Foundation Industry/University Cooperative Research Center at the University of Michigan and access to manufacturing facilities and sensor data provided by our automobile industry sponsors.

References

Asada, H., and By, A., 1985, "Kinematic Analysis of Workpart fixturing for Flexible Assembly with Automatically Reconfigurable Fixtures," *IEEE Journal of Robotics and Automation*, Vol. 1, pp. 86–94.

Ayres, R. U., 1988, "Complexity, Reliability, and Design: Manufacturing Implications," *Manufacturing Review*, Vol. 1, pp. 26–35.

Ceglarek, D., 1996, "Fixture Failure Diagnosis for Sheet Metal Assembly with Consideration of Measurement Noise," *Proceedings of the 2nd S. M. Wu Symposium*.

Ceglarek, D., and Shi, J., 1996, "Fixture Failure Diagnosis for Autobody Assembly Using Pattern Recognition," ASME JOURNAL OF ENGINEERING FOR INDUSTRY, Vol. 118, No. 1, pp. 55–66.

Ceglarek, D., and Shi, J., 1995, "Dimensional Variation Reduction for Automotive Body Assembly," *Manufacturing Review*, Vol. 8, No. 2, pp. 139–154.

Chryssolouris, G., Domroese, M., and Beaulieu, P., 1992, "Sensor Synthesis for Control of Manufacturing Processes," ASME JOURNAL OF ENGINEERING FOR INDUSTRY, Vol. 114, pp. 158–174.

Cowan, C. K., and Kovesi, P. D., 1988, "Automatic Sensor Placement for Vision Task Requirements," *IEEE Transactions on Pattern Analysis and Machine Intelligence*, Vol. 10, pp. 407–416.

Fukunaga, K., 1972, *Introduction to Statistical Pattern Recognition*, Academic Press.

Khan, A., Ceglarek, D., and Ni, J., 1998, "Sensor Location Optimization for Fault Diagnosis in Multi-Fixture Assembly Systems," ASME JOURNAL OF MANUFACTURING SCIENCE AND ENGINEERING, Vol. 120, No. 4, pp. 781–792.

Luo, R. C., and Lin, M. H., 1988, "Robot Multi-Sensor Fusion and Integration: Optimum Estimation of Fused Sensor Data," *IEEE Conference on Robotics and Automation*, Vol. 2, pp. 1076–1081.

Menassa, R. J., and DeVries, W. R., 1989, "Locating Point Synthesis in Fixture Design," *Annals of the CIRP*, Vol. 38, pp. 165–169.

Nelder, J. A., and Mead, R., 1965, "A Simplex Method for Function Minimization," *Computer Journal*, Vol. 7, pp. 308–313.

Powell, M. J. D., 1978, "A Fast Algorithm for Nonlinearly Constrained Optimization Calculations," *Numerical Analysis*, Lecture Notes in Mathematics, Springer-Verlag, Vol. 630.

Shekhar, S., Khatib, O., and Shimojo, M., "Object Localization with Multiple Sensors," *The International Journal of Robotics Research*, Vol. 7, pp. 34–44.

Tarabanis, K., Tsai, R. Y., and Allen, P. K., 1991, "Automatic Sensor Planning for Robotic Vision Tasks," *IEEE International Conference on Robotics and Automation*, Vol. 1, pp. 76–82.

Zussman, E., Schuler, H., and Seliger, G., 1994, "Analysis of the Geometrical Features Detectability Constraints for Laser-Scanner Sensor Planning," *International Journal of Advanced Manufacturing Technology*, Vol. 9, pp. 56–64.

Matlab: Optimization Toolbox User's Guide, 1994, The MathWorks, Inc.

J. D. Power Early Buyer Initial Quality Study, 1994, J. D. Power and Associates.